NEW SCIENCE FROM PULSED SOURCES

J L Finney, Rutherford Appleton Laboratory, Chilton, Didcot, OX11 0QX

1. Introduction

Four and a half years ago, at ICANS X in Los Alamos, we at ISIS were pretty pleased. ISIS was, for the first time, running at 100μA. More importantly, we were beginning to see new, exciting science coming from pulsed sources. In his summary talk at the end of that workshop Peter Egelstaff underlined the progress that had been made by announcing that pulsed sources had come of age[1].

Looking back from today, I believe that assessment was wrong. Understandably so, as when you are on a strongly rising curve whose future development you cannot know, it is difficult to assess your relative position on that curve. Pulsed spallation sources certainly had not come of age in 1988: at most, they were in early adolescence.

Since then, much has happened. ISIS has not only reached its design current of 200μA, but its reliability has increased significantly, and the number of scheduled instruments has more than doubled. The amount and variety of science being done each year has more than doubled, and many instruments have been improved beyond recognition, opening up the possibilities - and the realities - of more new science. We have learned much more how best to exploit the major advantages of pulsed sources. If we now look back from our present vantage point on the growth curve, at the quality and quantity of the science coming from pulsed sources, there is little comparison between the situation now and that 4½ years ago. Perhaps now, pulsed sources have come of age.

This review is therefore a celebration of pulsed source science. Using a necessarily very small selection of examples that I personally find particularly interesting, I will try to illustrate the advantages of pulsed sources through the new science they have made possible. I would emphasise this is a personal selection which inevitably must leave much out of interest and importance. I apologise for having to leave out so much.

2. The Advantages of Pulsed Spallation Sources

The conventional wisdom of pulsed sources tells us that the high energy (low wavelength) component in the delivered neutron spectrum is the key advantage. This allows us to perform inelastic scattering experiments with high energy transfer, for example in studying high energy magnetic excitations, as well as high momentum transfer elastic experiments which enables structural studies to very high resolution. These advantages are indeed powerful, allowing us to reach areas of science inaccessible to reactor neutrons. They are, however, only part of the story, as we have increasingly learned from recent experience. There are in addition other major advantages which all arise from the *pulsed* nature of the white beam of neutrons produced. In summary, these are:

- the high intrinsic resolution achievable in both space and time domains;
- a wide spectral range (meV→eV; 0.1Å → 20Å). This favours experiments exploring a wide dynamic range in both time and distance;
- the white beam allows fixed scattering geometries to be used. Not only is this ideal for background removal when working at 90° with pressure cells and reaction vessels but it also allows experiments to exploit other scattering angles for other optimisation reasons. Of particular importance are backscattering to maximise resolution in powder diffraction, and forward scattering to minimise inelasticity corrections in liquids;
- pulsed sources are essentially very low background sources: in essence the source is off when the data is collected. As signal/background ratio rather than intensity is often the determining quantity for a successful experiment, this low background allows more subtle effects to be seen more easily using by pulsed sources. This advantage is perhaps one whose potential value was not really appreciated before we started fully exploring the science that could be done.

In the examples that follow, the ways in which pulsed source instruments exploit the above advantages will be stressed.

3. High Energy Neutrons

Magnetic excitations provide one of the classic examples of the exploitation of high energy neutrons. One area which consequently has been opened up by pulsed sources is that of intermultiplet transitions in rare earth magnetic systems. As Fig 1 shows, only one transition ($^7F_o \rightarrow {}^7F_1$ of europium) is of low enough energy to be studied using reactors. The figure also shows some of the transitions that have been explored using pulsed neutrons. Non-dipolar allowed transitions have been observed up to 1800meV (thulium)[2], and measured inelastic structure factors have been shown to be in good agreement with calculations for praseodymium[3]. In contrast, for light rare earths, significant shifts are found for transitions to different L quantum numbers (e.g. $^3H_4 \rightarrow {}^3F_2$ in Pr) due to the screening of coulomb interactions by the conduction electrons, an effect which is even greater for 5f electrons. The technique also has applications to intermediate valence systems (e.g. Ce, Sm) and crystal field levels.

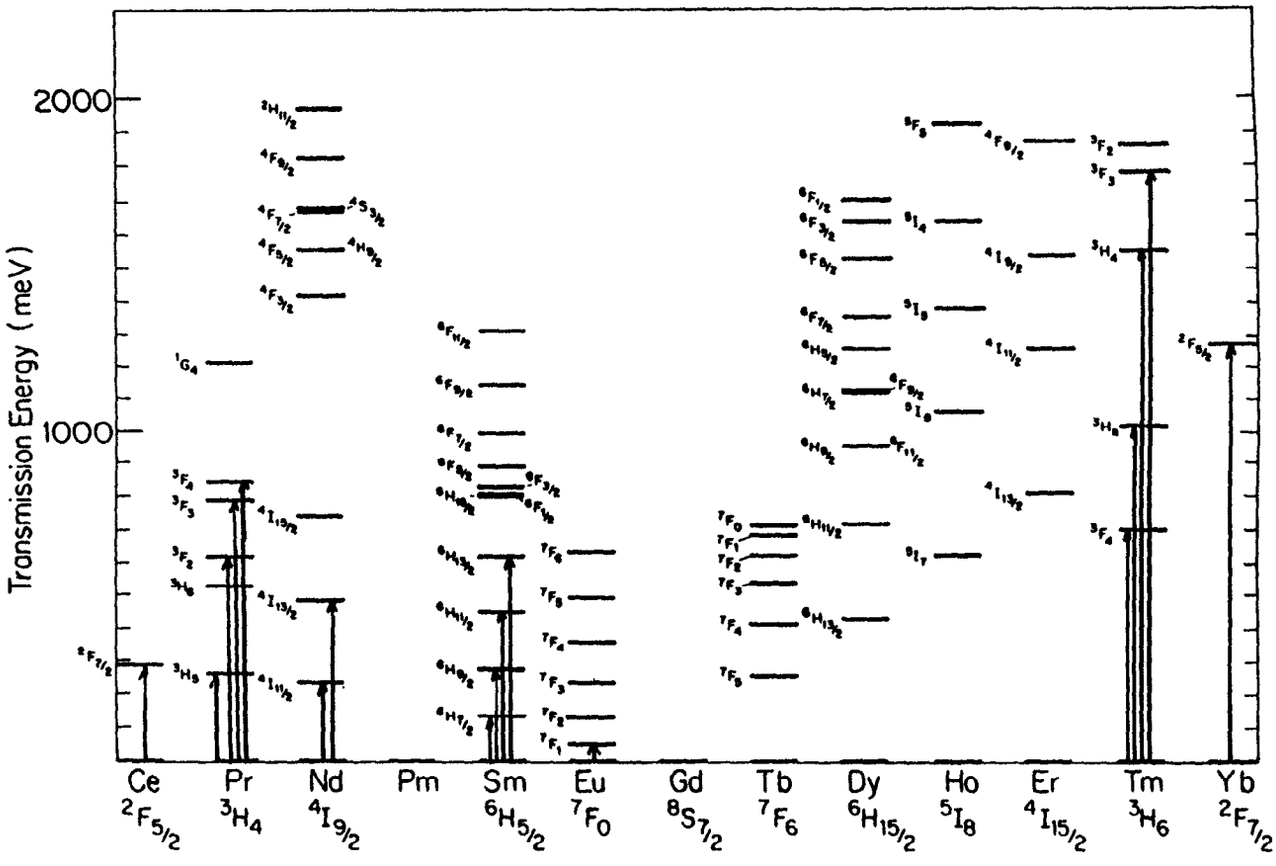

Figure 1: Intermultiplet levels in the rare earths. Transitions examined by neutrons are indicated. Only the $^7F_o \rightarrow {}^7F_1$ transition in Eu is accessible to reactor neutrons.

From the early days of pulsed neutrons, it was believed that they would be at their best in excitation studies of materials presented as powders rather than single crystals, and instruments were therefore optimised for powder work. As reactor-based instruments are restricted to energy transfers of below about 200meV, however, attempts were made to explore magnetic dispersion relations above the reactor limit, with considerable success as illustrated by work on cobalt[4] to the zone boundary at around 300 meV, and iron[5] and chromium[6] up to 550meV. As the dimensionality of the magnetic system is reduced, however, it becomes possible to exploit the detector geometry to good effect, work[7] which has enabled the magnetic dispersion in the magnetically two-dimensional high T_c parent compound La_2CuO_4 to be followed out to the zone boundary at 316meV (Fig 2), and the susceptibility of a Kagomé lattice system explored[8]. One dimensional magnetic systems are ideally suited to time of flight, as is illustrated by the case of $KCuF_3$[9]. Fig 3a illustrates the cut taken by incident 150meV neutrons while the results in Fig 3b indicate a quantum rather than a classical ground state. Fig 3b also underlines the low background, an advantage which is common - together with high intrinsic resolution - to most of these magnetic experiments.

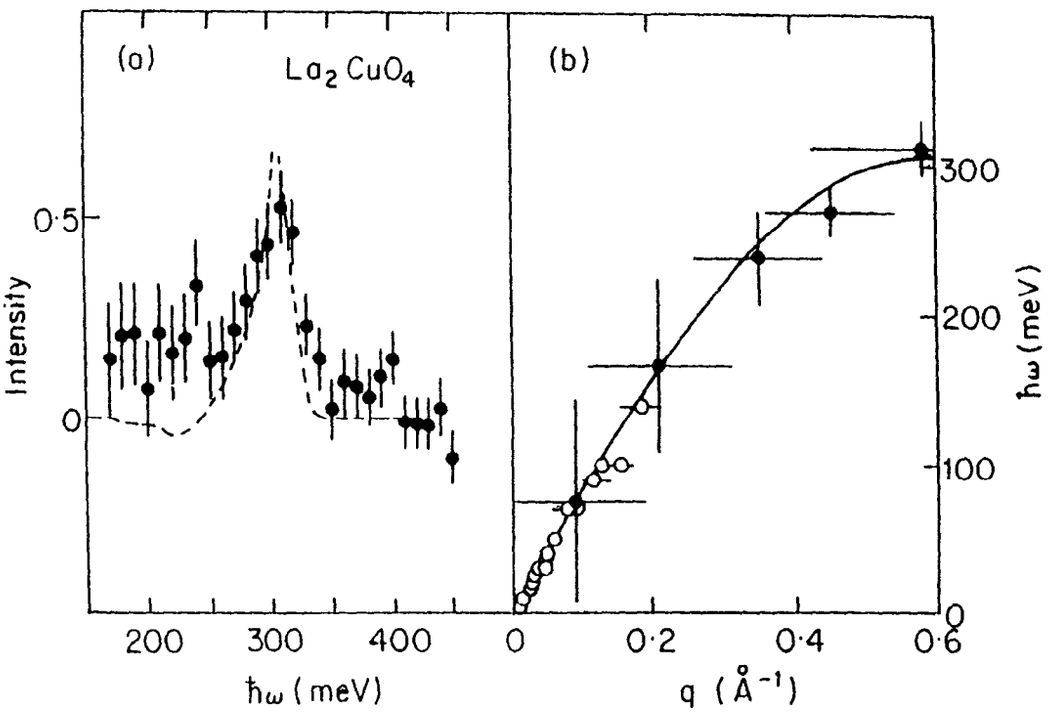

Figure 2: Magnetic excitation (left) and its dispersion (right) from a composite single crystal of La_2CuO_4. The response can be seen to be followed to the zone boundary at 316 meV.

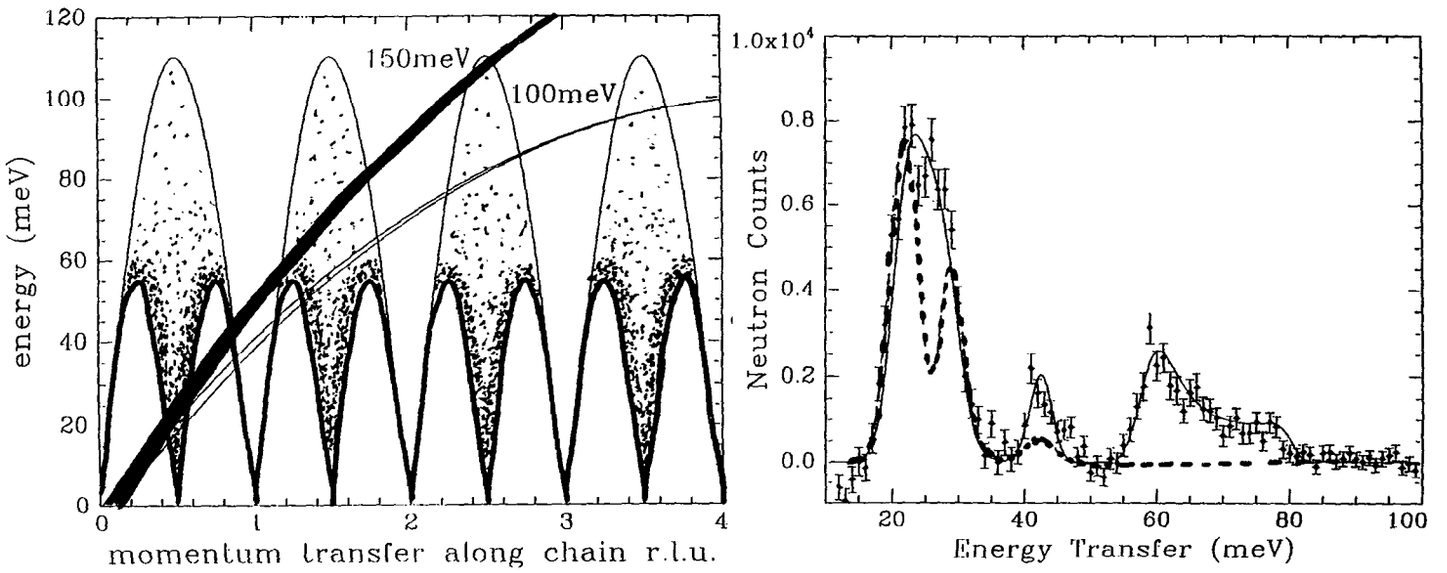

Figure 3: Magnetic excitations in the one-dimensional $KCuF_3$ system. The dotted line in 3(b) indicates the expected response for the 150 meV cut (Fig 3(a)) for a classical ground state. The actual results indicate clearly a quantum ground state.

Moving away from magnetic systems and to even higher energy transfers, we come to the completely new area of electron volt spectroscopy. In effect, by scattering neutrons with very high energy and momentum transfer, we can probe directly the wave function. Here, a long standing problem has been to observe the Bose condensate in liquid ^{4}He, and a series of experiments at IPNS and ISIS continue to tackle this problem. Fig 4 summarises the IPNS results[10], which, after correction for final state effects, are consistent with a Bose condensate fraction of about 9% in the superfluid at T=0K. Work on the new eVS instrument at ISIS allows higher momentum transfers to be accessed, and hence a closer approach to the impulse approximation. A significant amount of work has been done to probe the hydrogen wave function in hydrogen bonded systems[11] - both along and normal to the bond - and although still in the early stages of development, these studies promise much new and important information on a chemically and biologically very important interaction.

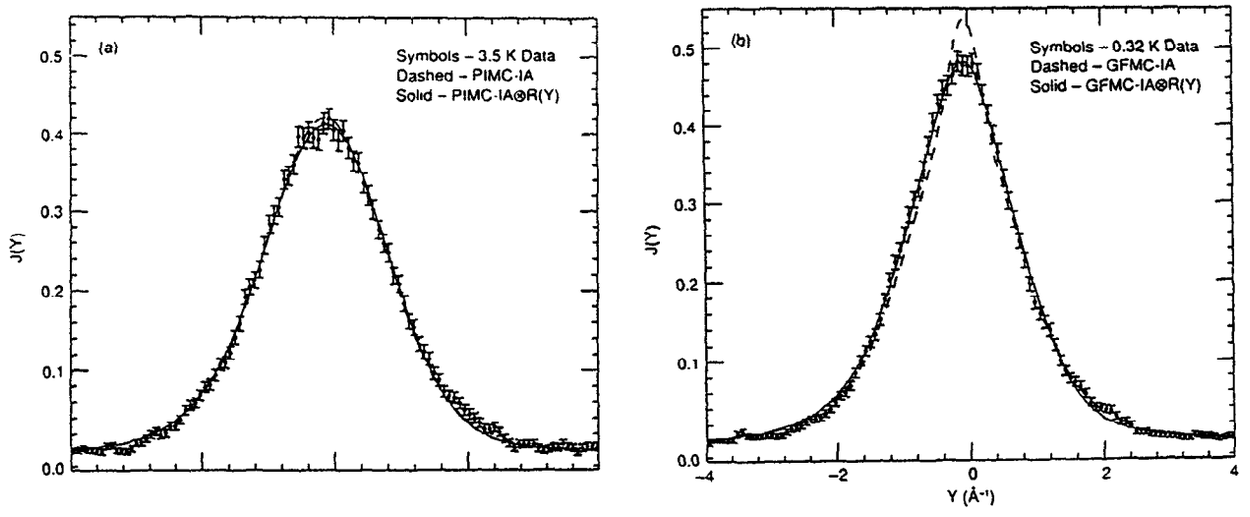

(a) (b)

Figure 4: The Compton profile for (a) normal liquid helium at 3.5 K and (b) superfluid helium at 0.35 K as a function of the scaling variable Y [=(M/Q)($\omega - \omega_r$), where ω_r {=Q^2/2M} is the recoil energy]. The dashed lines are the theoretical predictions with instrumental resolution taken into account. The solid lines include final state effects in the comparison.

4. Very High Spatial Resolution

In pulsed source instruments, the spatial resolution achievable increases with time of flight, and hence with moderator-detector distance. The resolution achievable is illustrated well by the typical powder pattern taken from HRPD, situated nearly 100 m from the ISIS target, shown in Fig 5. Not only is the resolution, at $\Delta d/d \sim 4 \times 10^{-4}$, unmatched by any other neutron powder diffractometer, but, again characteristic of pulsed source instruments, this resolution is essentially constant with d-spacing. Thus, as a powder pattern is essentially a set of Fourier components of the crystal structure, as the number of "reflections" increases, the precision with which a structure can be refined also increases. Coupled with the wide dynamic range over which this high resolution is achievable, high resolution neutron powder instruments such as HRPD have little short of revolutionised powder diffractometry, allowing us to do science with powders that previously was not possible.

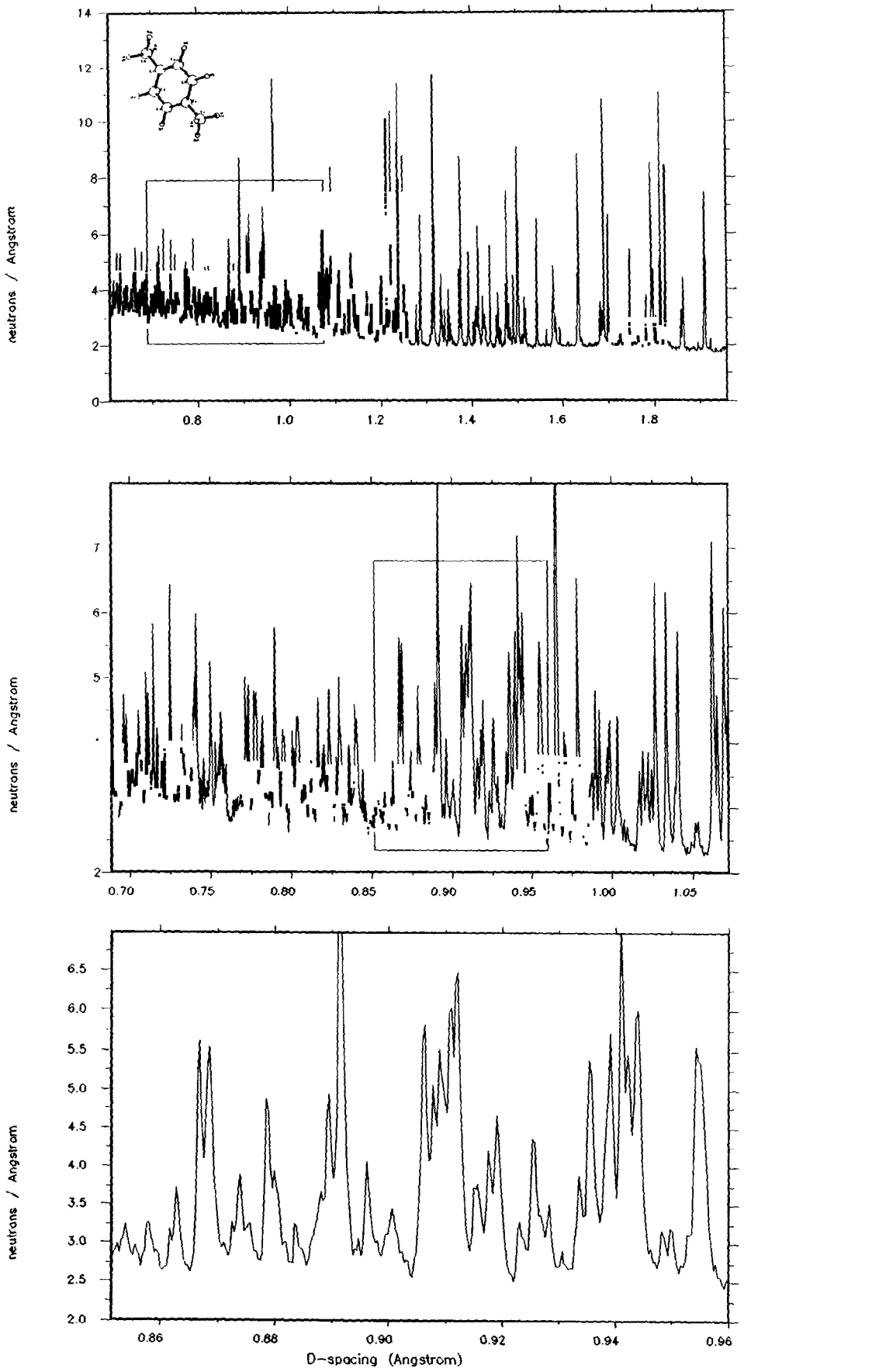

Figure 5: The powder diffraction of p-xylene taken on HRPD, illustrates both the very high - and constant - resolution, and the bandwith achievable in a single "shot". The two lower figures show blown-up the region framed in the figure above.

For example, more complex structures can be refined, and more subtle effects observed. An obvious example is structural studies of high temperature superconductors, where pulsed sources continue to make major contributions. Here, in addition to the work at ISIS,[12] the careful, thorough studies undertaken at Argonne are particularly noteable[13]. Secondly, we can now solve structures with powders and perform refinements of a quality that previously required single crystals. The "canonical" example is the refinement of the anistropic temperature factors of benzene from HRPD data[14], the comparison of which with single crystal measurements is shown in table 1. Within the quoted errors, the two sets of results are essentially the same. For this experiment, the standard deviations of the powder data are perhaps three times those of the single crystal figures, though longer data collection times would reduce this difference: in this case, the powder data was taken in 12 hours, the single crystal data over 3 weeks.

Time-of-flight powder neutron diffraction (4K)

HRPD $0.281\ Å^{-1} < \sin\theta/\lambda < 0.824\ Å^{-1}$

Atom	B_{11}	B_{22}	B_{33}	B_{23}	B_{13}	B_{12}
C1	77 (7)	42 (6)	87 (7)	1 (5)	5 (5)	-3 (4)
C2	71 (7)	58 (7)	68 (6)	9 (4)	26 (5)	12 (4)
C3	83 (7)	57 (7)	92 (7)	0 (5)	18 (5)	-1 (4)
D1	218 (8)	121 (7)	267 (9)	19 (5)	22 (6)	31 (5)
D2	170 (8)	212 (8)	225 (9)	-2 (6)	120 (6)	33 (5)
D3	241 (9)	155 (8)	214 (8)	75 (6)	66 (7)	-20 (5)

Single crystal neutron diffraction (15K)

BNL - 4-circle $1.0499\ Å^{-1}$. $0.403\ Å^{-1}$. $< \sin\theta/\lambda < 0.780\ Å^{-1}$

Jeffrey et al. Proc. R. Soc. Lond. **A 414** 47-57 (1987)

Atom	B_{11}	B_{22}	B_{33}	B_{23}	B_{13}	B_{12}
C1	79 (2)	67 (2)	88 (2)	4 (1)	7 (2)	6 (2)
C2	74 (2)	81 (2)	79 (2)	0 (2)	17 (2)	9 (2)
C3	81 (2)	75 (2)	82 (2)	10 (1)	14 (2)	-3 (2)
D1	224 (3)	114 (2)	239 (3)	12 (2)	25 (2)	46 (2)
D2	183 (2)	204 (3)	208 (3)	-8 (2)	88 (2)	35 (2)
D3	214 (3)	171 (2)	199 (3)	58 (2)	61 (2)	-18 (4)

Table 1: Anistropic temperature factors ($10^4 Å^2$) for deuterated benzene.

This ability to work with powders rather than single crystals promises to be a major step forward: growing the single crystals is often the rate determining step in a structural study, and often - e.g. in new materials synthesis such as zeolites - not possible. In elucidating drug structures, necessary if we are to determine the drug shape for correlation with its biological activity, pulsed neutron powder diffraction is beginning to make significant contributions: active drugs are often only available as powders, and may lose their activity in different crystal forms or when grown as single crystals. A recent example from HRPD is that of the neurotransmitter dopamine, for which accurate positions of both backbone and the interaction-important hydrogen atoms are obtained[15].

High resolution pulsed neutron diffraction has solved the low temperature structure[16] of Buckminsterfullerene, C_{60}. The high resolution also led to the uncovering of a dynamical phase transition through measuring to high precision the lattice constant as a function of temperature[17]. Fig 6 shows this temperature variation, in which each data point was measured in 15 minutes. In addition to the known transition around 260K, a second transition occurs at around 85K. Fig 7 illustrates the overall nature of these transitions. Above the higher temperature one, the molecules rotate with no preferential rotational axis, while below the 260K transition, rotation becomes restricted to a single axis. Below 85K, this motion freezes out, and the system adopts the low temperature structure. The quality of the powder data is further demonstrated by Fig 8, which shows how the "ideal" mutual orientation of nearest neighbour C_{60} molecules (pentagon facing 6:6 bond: see Fig 8) is not fully achieved in the low temperature structure. Refining occupancies shows that ⅛ of the nearest - neighbour configurations do not adopt this "ideal": hence the zero temperature intercept of 0.833 in Fig 8.

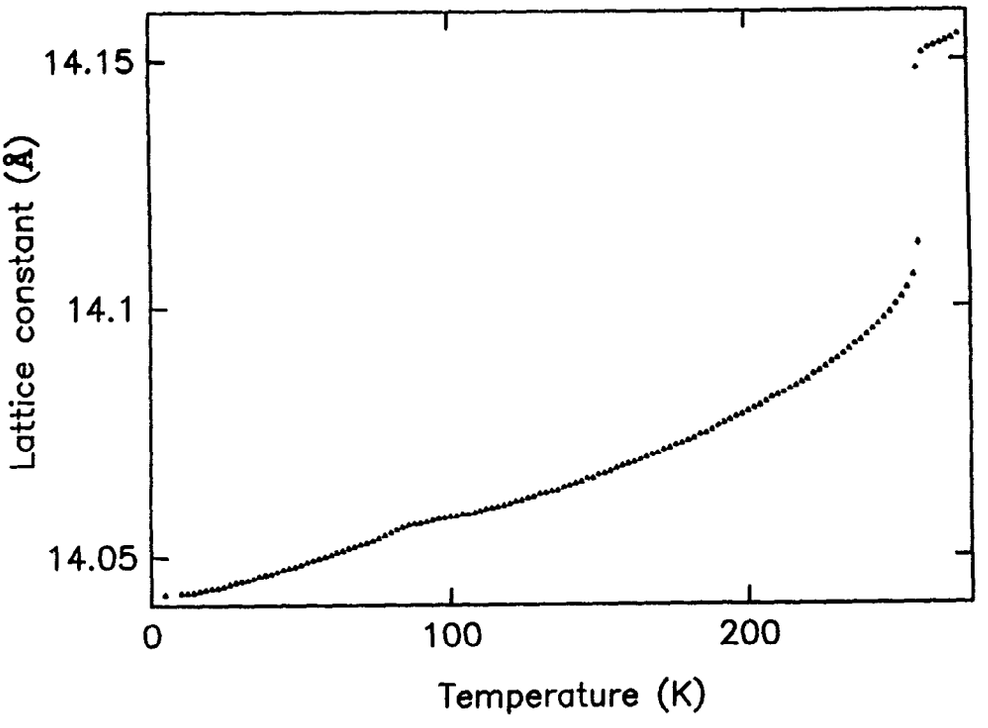

Figure 6: The temperature variation of the lattice parameters of C_{60}, showing transitions at around both 260K and 85K

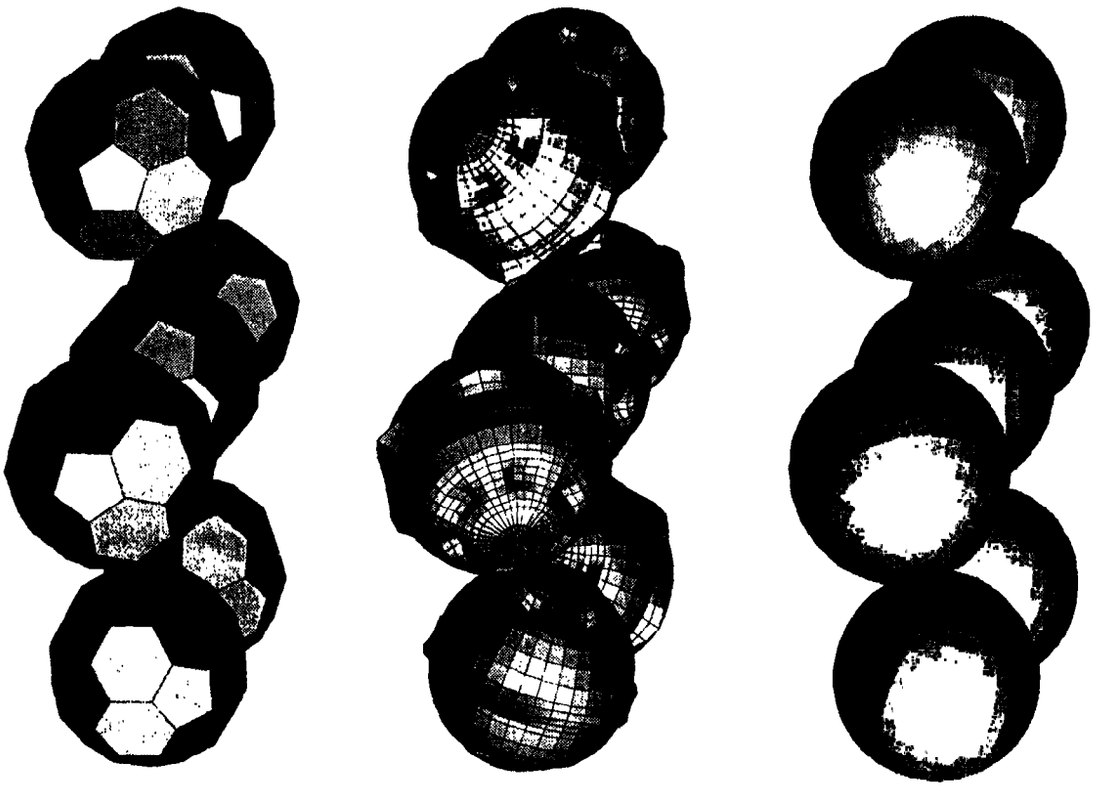

Figure 7: Above around 260K, C_{60} molecules appear to rotate around no preferential axis (right). Below the upper transition, rotation becomes restricted to a single axis (centre) while below about 85K the low temperature structure is adopted (left).

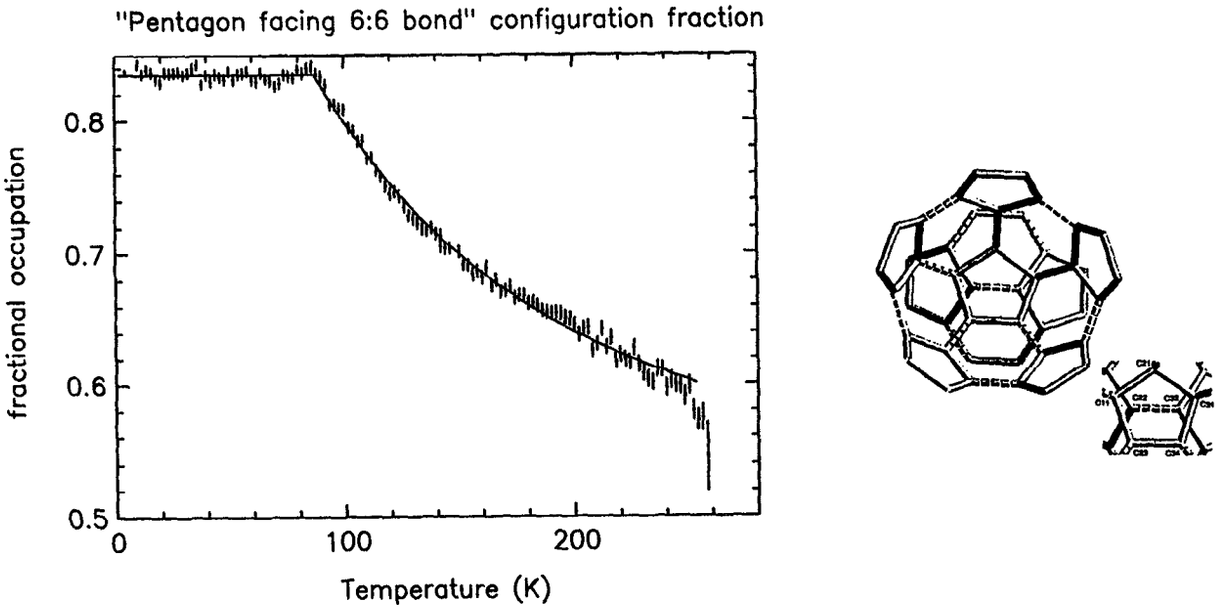

Figure 8: Even below 85K the low temperature structure is not fully ordered. Only $^5/_6$ of the local configurations (0.833) are in the "ideal" configuration shown.

Crystallography is recognised to be a very powerful technique, and when allied to pulsed neutrons can be even more powerful, as the above has underlined. It does however have limitations, and it is worth digressing a little to discuss this point. Broadly speaking, a crystallographic structure will give average positions of molecules, with "temperature factors" which themselves can often give us some information on disorder in the structure. This averaging of atomic position can, however, hide mechanistically useful information which other techniques can reveal. An example from IPNS - with similar work progressing at LANSCE - again concerns high T_c materials[18]. In the La_2CuO_4 system, crystal structure determination tells us the CuO_4 conduction layer is planar. Using the crystal co-ordinates, we can calculate the distribution function of pairs of atoms (the probability of finding an atom at a given distance from any other atom), and the result for $Nd_{2-x}Ce_xCuO_4$ is given by the solid line in Figure 9. This distribution function can also be obtained by diffraction measurements, and in fact this is the standard way of looking at liquid and glass structures using neutrons or x-rays. The experimental results for $Nd_{2-x}Ce_xCuO_4$ both above (50K) and below (10K) the superconducting transition are also shown in Figure 9, and there are clear differences both from the "average" structure given us by crystallography and between the superconducting and non-superconducting states. The local structure is thus considerably different from the average crystallographic structure, and changes in local structure can be associated with the onset of superconductivity. Structural modelling indicates that the observed differences can be explained partly by oxygen atoms being displaced by small amounts perpendicular to the CuO_4 plane. With respect to this pair distribution technique, we should note that the degree of detail observable - the resolution - increases with increasing momentum transfer Q, and increased Q in turn requires short wavelength neutrons. This again underlines the power of pulsed spallation neutrons, where this high energy component is present in the incident spectrum.

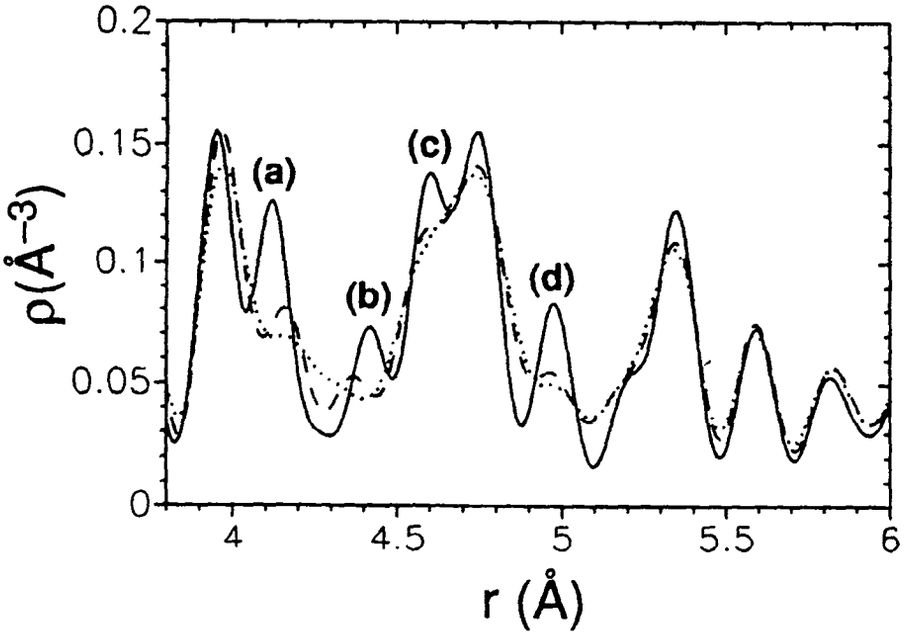

Figure 9: Calculated-PDF (solid line) of the crystal (T') structure superimposed on the data-PDFs from the 50K (dotted line) and 10K (dashed line) of the superconducting sample.

5. Fixed Scattering Geometry

By measuring diffraction from a sample at 90°, the collimation of incident and diffracted beams can be optimised to remove - in essence completely - parasitic scattering from the sample environment, which is perhaps a heavy pressure cell or chemical reaction vessel. This is illustrated dramatically by Fig 10, which shows powder patterns of ice VIII taken on a reactor source (ILL)[19] and at 90° at IPNS[20]. Although the reactor pattern looks superficially good, what is seen is largely scattering from the sample environment, which very much dominates the ten or so sample peaks that are marked. In comparison, the IPNS data show only the sample peaks - those from the pressure cell have been collimated out.

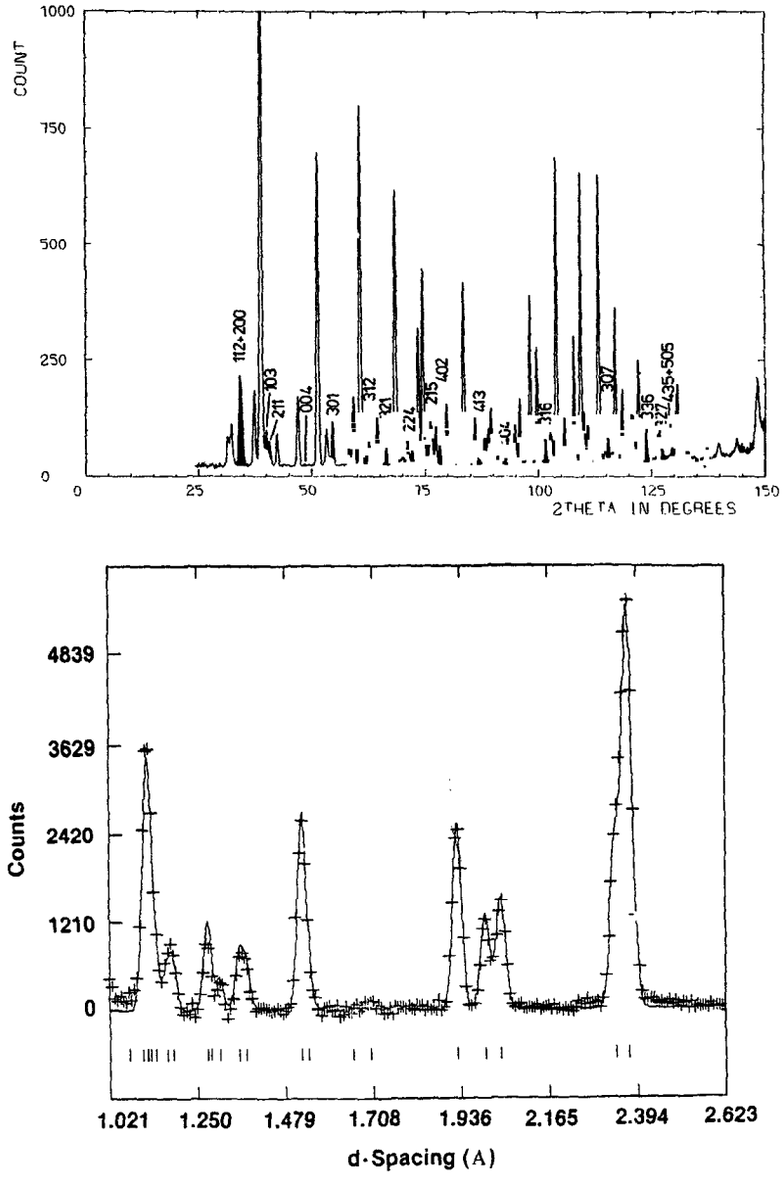

Figure 10: The powder diffraction patterns of ice VIII taken on a reactor source (ILL-upper) and a pulsed source (IPNS-below). Only the labelled peaks in the upper figure originate from the sample. The pressure cell peaks have been collimated out in the pulsed neutron pattern.

Small wonder, therefore, that high pressure studies on pulsed sources are expanding rapidly. A particularly interesting study from IPNS is on the high T_c material $Tl_2Ba_2CuO_6$, for which T_c depends on the oxygen concentration[21]. Applying pressure at room temperature also changes the critical temperature, while applying the same pressure changes at low temperature has very little effect on T_c. Preparing samples using different paths in (p,T) space (e.g. applying up to 6kbar at 295K and then cooling; cooling before applying pressure; intermediate paths by applying some pressure at 295K, cooling, and then increasing the pressure to 6kbar), crystallographic measurements showed clearly that the resulting structure depends on the path taken in (p,T) space. This work suggested that the interstitial oxygen defect mobility is reduced at reduced temperatures, and also perhaps that applying pressure at room temperature leads to defect ordering.

90° scattering geometry is being further exploited in a Paris-Edinburgh collaboration which is developing neutron high pressure techniques to reach much higher pressures than the present normal upper limit of around 25kbar[22]. Working with an anvil arrangement, data has been taken at pressures up to 250kbar, extending the accessible pressure range by an order of magnitude. In recent work at ISIS[23], refineable patterns from ice VIII were taken at 101kbar which gave a precision on the O-D bond length the same ($\pm$ 0.003Å) as at 25kbar. As this cell enters service as a user facility, further new advances are expected in high pressure exploitation.

Fixed geometry scattering is also exploited in making *in-situ* strain measurements. The strain is reported by small shifts in Bragg peak positions, so high resolution is also desirable. By measuring scattering from an appropriately aligned sample, strain both normal and parallel to the applied load can be measured simultaneously by taking data at both + and - 90° scattering positions. With appropriate collimation, strain can be measured pixel by pixel to give the spatial variation within the sample. However, using pulsed neutrons, strain can be measured for different lattice planes, again at the same time and orientation.

An example of work from LANSCE on a metal-matrix composite - aluminium reinforced with SiC whiskers - is shown in Fig 11, where the experimental results are compared with the results of finite element calculations[24]. For the parallel strain, theory and experiment are still some way apart, while for the normal strain, there is better agreement with the average strain deduced from profile refinements of the whole pattern However, in the latter case, there is a strong hkl dependence, which not only gives more detailed information, but also indicates the danger of drawing conclusions from the one hkl peak that is normally used in reactor studies of residual strain.

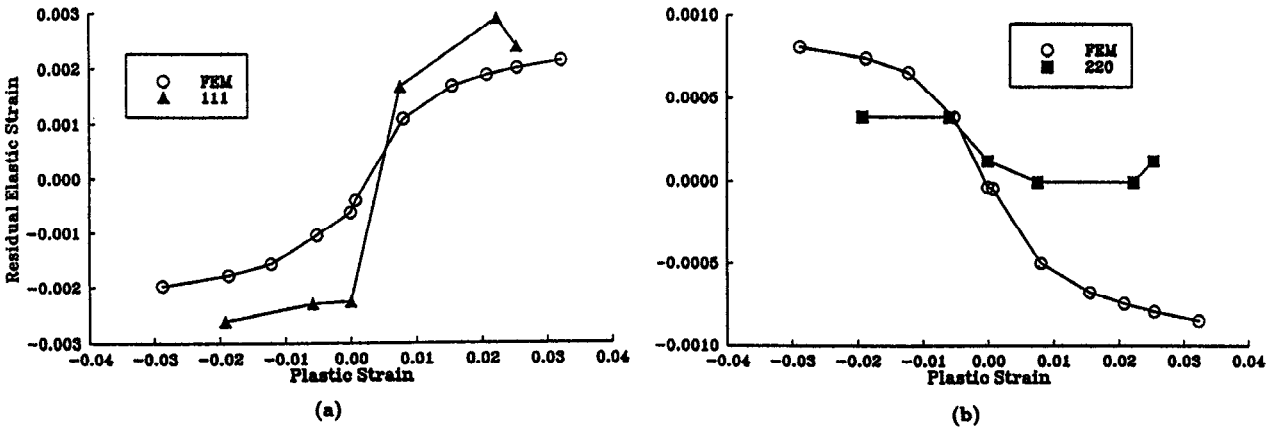

Figure 11: Measured and predicted values of average residual elastic strains in the matrix (a) parallel and (b) perpendicular to the deformation axis, from a 15% whisker composite strained in tension to a plastic strain of 0.018, deformed in compression and then unloaded.

These techniques are very much still under development: they promise much in evaluating the performance of increasingly complex engineering materials.

Although I shall say little further on the matter, structural studies of liquids and glasses using pulsed neutrons have also resulted in significant progress in the field. As mentioned above in the discussion of pair distribution studies of high T_c materials, the much greater momentum transfer range accessible using the hot neutrons from a pulsed spallation source enables significantly greater structural detail to be obtained. When dealing with light atoms, pulsed neutrons have even greater advantages which result from working at "fixed" scattering geometry, in this case at low angles. This minimises troublesome inelasticity corrections and results in much improved data quality from such systems. These advantages have been exploited particularly in studies of aqueous solutions using hydrogen-deuterium and other atom substitution, and have told us a great deal about not only the hydration of charged, polar and non polar groups, but also how the water is or is not perturbed close to such groups[25].

6. Time Dependent Studies and Time Structure

The white beam of neutrons produced by a pulsed source enables the whole diffraction pattern to be measured simultaneously, rather than having to scan step by step as a function of scattering angle as is necessary on a standard monochromatic instrument on a reactor source. The ability to see the whole diffraction pattern build up over a relatively short time has natural advantages for time-dependent studies. Such work is of course possible on a reactor using multidetectors, but the white pulsed beam is more flexible for such studies, and, depending on neutron intensity, it is in principle possible to perform time dependent measurements on time scales as low as a few - or even perhaps a single - neutron pulse.

An example from Dubna of time resolved studies over intervals of 5 minutes concerns the synthesis of the yttrium 123 superconductor $YBa_2\ Cu_3\ O_x$[26]. Fig 12 shows the intensities of particular diffraction peaks identified with different compounds at five minute intervals. The interesting result here is that the synthesis proceeds not directly from the starting materials, but through three intermediate phases which coexist prior to the formation of the Y-123 end product. With intense pulses, it is easy to see how the time interval can be reduced, and a glimpse of the possibilities is given in Fig 13, which shows a diffraction pattern of molybdenum powder from (lower figures) 300 pulses (1 minute) and (upper figure) a single pulse. The diffraction pattern is clearly visible in the single pulse measurement, showing that in favourable cases single pulse measurements are already possible.

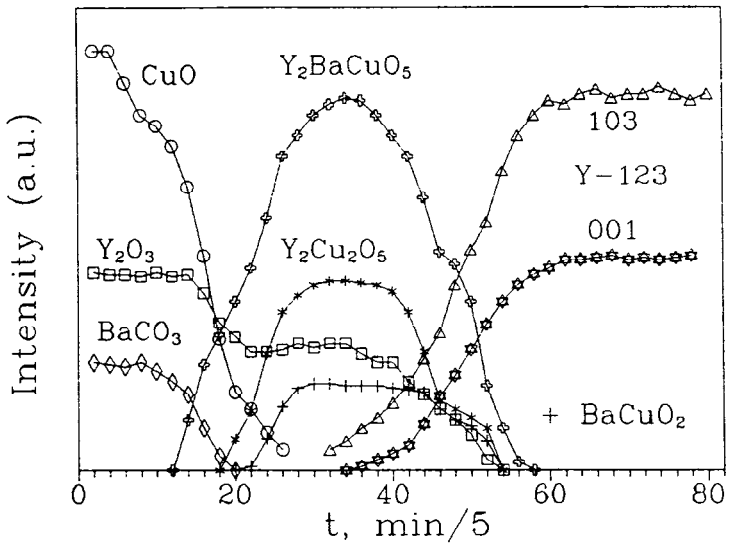

Figure 12: The intensities *vs* time of some diffraction peaks (relative units) which belong to different compounds during the synthesis of $YBa_2Cu_3O_x$ from raw materials Y_2O_3, CuO and $BaCO_3$. Three intermediate phases Y_2BaCuO_5, $Y_2Cu_2O_5$ and $BaCuO_2$ coexisted before the formation of Y-123 started.

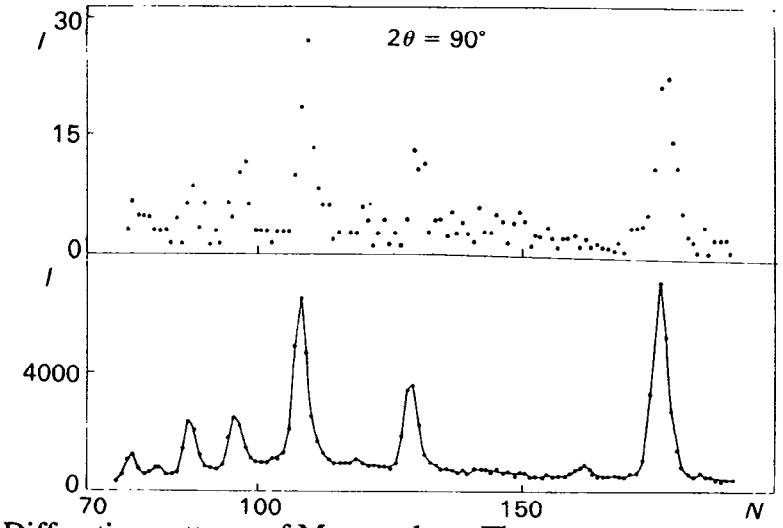

Figure 13: Diffraction patterns of Mo powder. The upper pattern was recorded in 1 pulse of the Dubna pulsed reactor, the lower one in 1 min (300 pulses of the pulsed reactor).

Also possible, but so far only exploited in limited degree, are "stroboscopic" - type measurements in which the sample is perturbed periodically by an external agent, in phase with the neutron pulse. This might be necessary when, as for example with very high magnetic fields, the sample perturbation cannot be obtained continuously and must therefore be pulsed. Pulsed magnetic field measurements have been pioneered at KEK, with some impressive results[27]. A recent example is the magnetic transition in the quasi one dimensional antiferromagnetic $CsCuCl_3$[28]. This system was expected to reveal enhanced quantum fluctuations in its magnetic properties, and the data taken on the magnetic transition at about 12 Tesla could be explained in terms of these fluctuations.

Another use of the time structure is illustrated by a recent experiment on ISIS. This addresses a system in which a phase transformation is restarted periodically and, consequently, time-resolved measurements on a millisecond time scale are possible. Rb_2ZnCl_4 has a ferroelectric transition close to 193K which is accompanied by a structural transition from incommensurate to commensurate. In the experiments on PRISMA - described in more detail elsewhere in these proceedings[29] - 5 pulses from ISIS are in effect ganged together, and an electric field applied with a frequency of 5Hz. The commensurate and incommensurate Bragg peaks can then be observed, and their relative intensities followed as a function of time at (variable) fixed temperature. The results at 193.5K are shown in Fig 14, and suggest a lag of a few milliseconds after applying or removing the field before the transition starts and, at this temperature, the transformation going to about 90% completion in the 100 ms time frame. Changes over periods as short as a few milliseconds can clearly be observed. Although this kind of use of pulsed sources has frequently been suggested, I believe this is the first effective demonstration of its implementation. Clearly it is capable of further development, for example to measure the kinetics of phonons in conjunction with a phase transition.

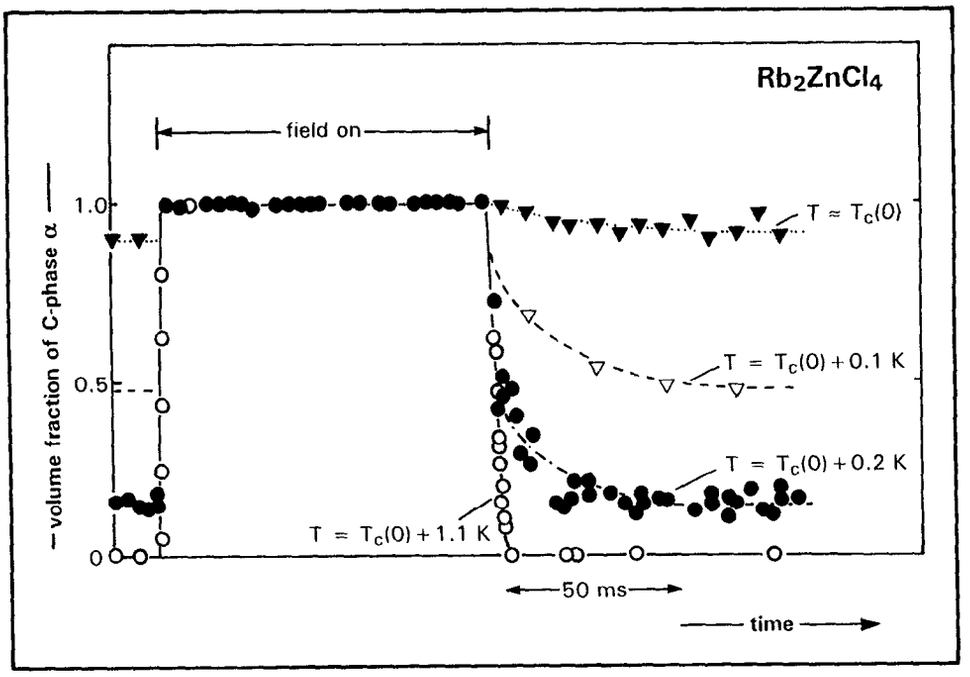

Figure 14: The relative intensities of the commensurate and incommensurate Bragg peaks during the ferroelectric transition in Rb_2ZnCl_4.

Pulsed spallation neutron sources also produce a variety of other particles. At ISIS for example, both neutrinos and muons are exploited, important aspects of their exploitation being again the time structure and associated low background.

In the KARMEN neutrino experiment at ISIS[30], three types of neutrinos are produced through pion decay as follows:

$$\pi^+ \xrightarrow[26\text{ns}]{} \mu^+ + \nu_\mu$$
$$\mu^+ \xrightarrow[2.2\mu\text{s}]{} e^+ + \nu_e + \bar{\nu}_\mu$$

Clearly, the ν_μ is produced in a time window different from that in which the ν_e and $\bar{\nu}_\mu$ are formed, and hence they can be distinguished. In addition to searching for neutrino oscillations, cross-sections for some neutrino-induced interactions are being measured, for which the time structure is again crucial. An example is the neutral current nuclear excitation $^{12}C(\nu, \nu')^{12}C^*$, in which the resulting 15.1MeV γ is measured as a signature of the C* decay. Fig 15 shows the measured events spectrum, and the looked-for γ peak is clearly visible between 11 and 16 Mev. The resulting experimental cross-section - which is a new measurement - of [11.2 $\pm$ 1.3 (statistical) $\pm$ 1.0 (systematic)] x $10^{-42}cm^2$ is within the range of the theoretical prediction [9.9 - 11.5] x $10^{-42}cm^2$.

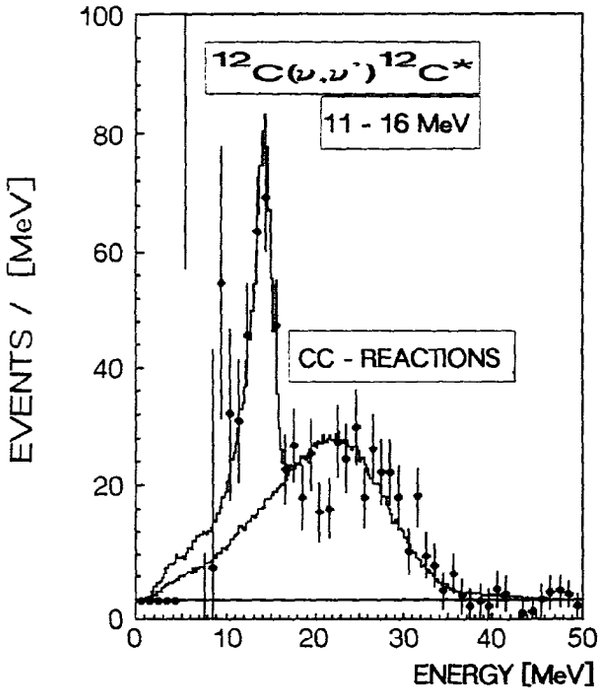

Figure 15: The events spectrum for the neutral current nuclear excitation of ^{12}C. The C* decay signature - 15.1 MeV γ - is clearly visible in a peak between 11 and 16 MeV.

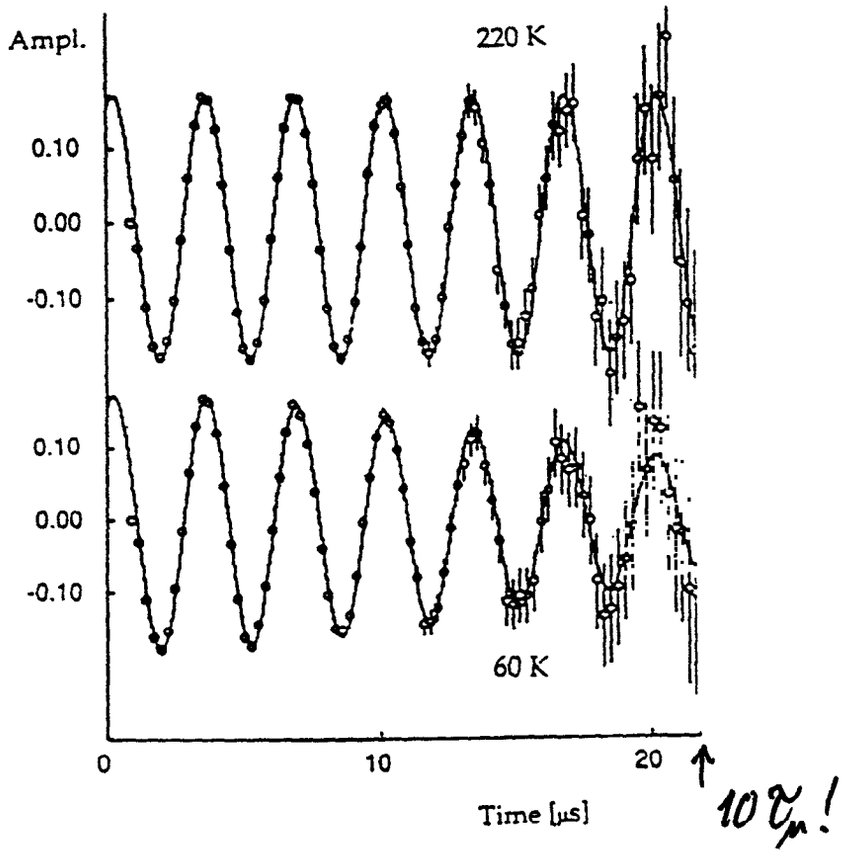

Figure 16: The muon spin rotation signals in Pt at two temperatures, showing damping at the lower temperature. Note that signals can be fitted to beyond 10 muon lifetimes.

KEK and ISIS both have pulsed muon sources. Here again the property of interest which gives rise to high quality spectra is the virtual absence because of the time structure of a background signal. This is illustrated in Fig 16 by muon spin rotation signals in platinum[31]. The signals can be fitted to beyond 10 muon lifetimes ($10\tau_\mu \simeq 22\mu s$), which is unprecedented in the μSR literature. In this case, it allows the weak damping at the lower temperature to be discerned. The temperature dependence of the fitted line width shows "textbook" behaviour, indicating static muons below about 100K and motional narrowing indicating the onset of diffusion at higher temperatures. The motion is by thermally activated hopping, with no sign of enhanced quantum diffusion at low temperature, in contrast to Cu and Al which also have f.c.c. structure. The static line width for muons in Pt is an order of magnitude less than in Cu, confirming that the dynamic range for such measurements is effectively extended by over a decade by the pulsed nature of the source.

7. Cold Neutrons

Just as the "old" conventional wisdom about pulsed sources asserts that hot neutrons are the major advantage, so also it says that cold neutron studies are not effectively performed on pulsed sources. And whereas the assertion on hot neutrons is found to be merely incomplete - as illustrated by many examples above - the statement on cold neutrons is demonstrably wrong. Experience at all operating pulsed sources has clearly demonstrated that they are indeed powerful engines for cold neutron diffraction and spectroscopy.

For example, reflectometry has been an outstanding success at pulsed sources world-wide. Taking advantage of the fixed geometry (which eases corrections) and low backgrounds, a tremendous amount of new science has been performed over a very wide range of chemistry, physics, materials science and biology. Through reflectometry, we have our first reliable view of the structure of surfactants at the air-liquid interface, polymer interdiffusion, and thin magnetic layers to list but three of a myriad possible examples. Moreover, the field is far from static, with new developments for example in liquid-liquid and liquid-solid interface studies, and exploration of the non-specular scattering. More comprehensive reviews can be consulted for detailed examples[32].

High resolution spectroscopy with pulsed cold neutrons has been a major success, led by the IRIS instrument at ISIS and LAM-80 at KEK. Both instruments have seen major improvements which have improved greatly the quality of spectra and opened up new areas. An example from KEK explores rotational tunnelling of a methane monolayer adsorbed on a graphite surface[33]. There are three spin species of the CH_4 molecule, the interconversion between them being forbidden. However, adding oxygen as a magnetic impurity catalyses the conversion. Fig 17(left) shows the non-equilibrium tunnelling spectrum at 0.32K, while fig 17(right) shows the effect of doping with 1% O_2: the impurity catalyses the attainment of equilibrium. Further work is planned to follow the time evolution to clarify the spin conversion mechanism.

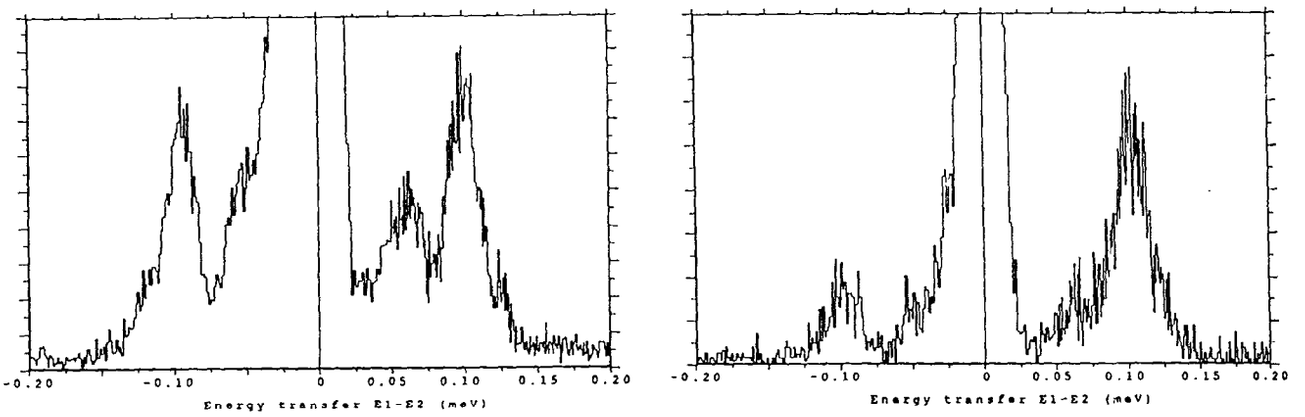

Figure 17: Rotational tunnelling spectra obtained at 0.32K for a CH_4 monolayer on graphite. Left: pure monolayer; right: doped with 1% O_2.

Because neutrons can be used to probe both structure and dynamics of a given system, lipservice has often been paid to the possibility of performing simultaneous elastic and inelastic experiments on the same sample. This is particularly appropriate for systems which are prepared in-beam, and when the conditions of production cannot necessarily be reproduced exactly for experiments on different instruments. Because a diffraction pattern can be measured in a single direction on pulsed sources, simultaneous diffraction and spectroscopy measurements are particularly suited to them. An example from IRIS - in which the diffraction detector was a single helium tube - is shown in Fig 18. The system is cesium intercalated graphite, to which is added increasing amounts of ammonia, which interacts directly with the cesium. Before adding NH_3 (x=0.0), two d-spacings show in the diffraction

pattern, and only the elastic line is evident in the inelastic spectrum. As NH_3 is added, an additional diffraction line begins to appear, while the inelastic spectrum shows a pair of tunnelling lines plus the free rotor line. Above x=0.42, further changes occur in both diffraction and inelastic signals, and these changes continue up to the maximum x=1.90. An interpretation of what is happening can be offered which involves the information obtained from the diffraction pattern[34].

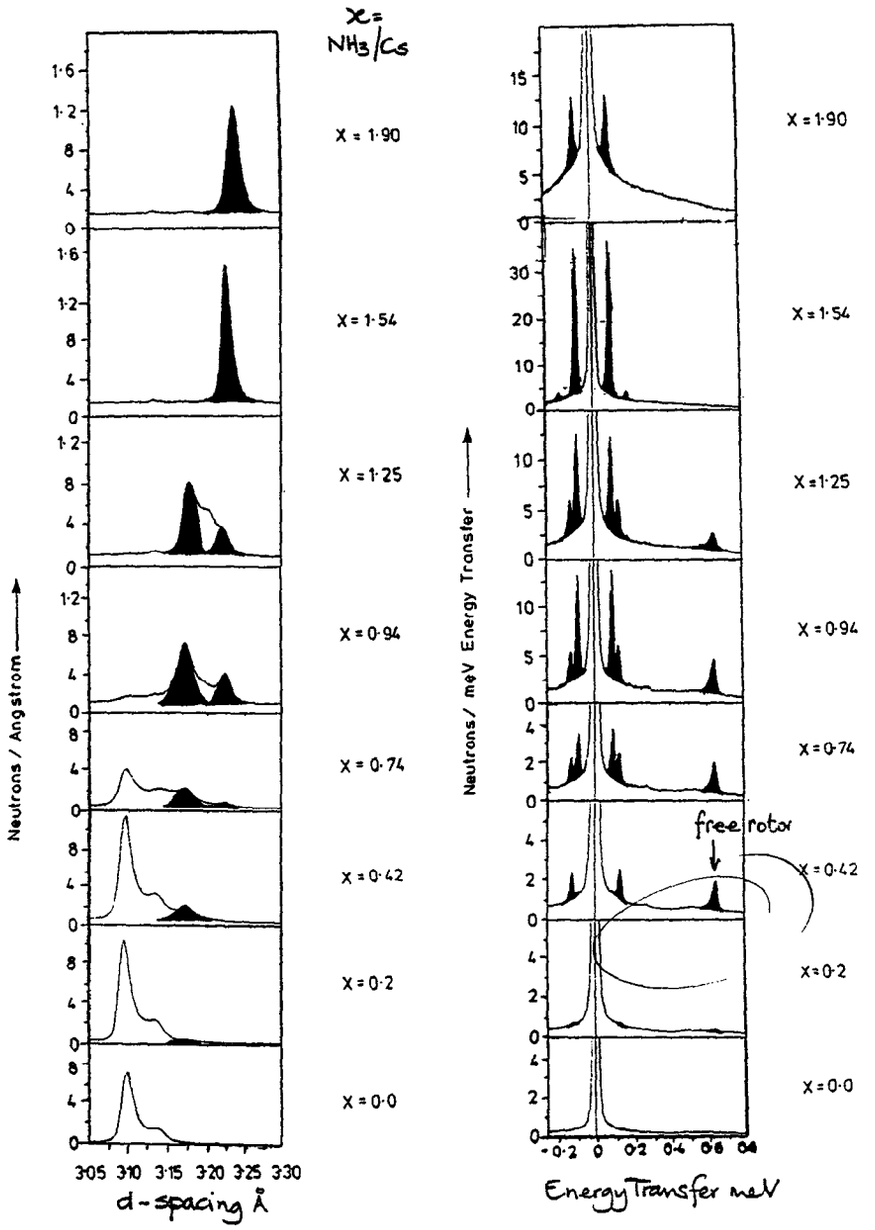

Figure 18. The tunnelling spectrum of Cs-intercalated graphite as the fraction x of NH_3 is increased (right). The left hand figure shows part of the diffraction pattern taken simultaneously, and assists in interpreting the tunnelling results.

A further example of the power of cold neutrons on pulsed sources is again from IRIS, but using only the diffraction detector to do long d-spacing crystallography. Figure 19 shows the pattern for $FeVO_4$ at 5K, with the magnetic peaks labelled. This spectrum has a good resolution of $\Delta d/d \sim 2.5 \times 10^{-3}$, uses wavelengths up to 18Å, and was taken in 4 hours. It is therefore possible to follow the two magnetic transitions as the temperature is raised, and more details of this are given elsewhere in these proceedings[35].

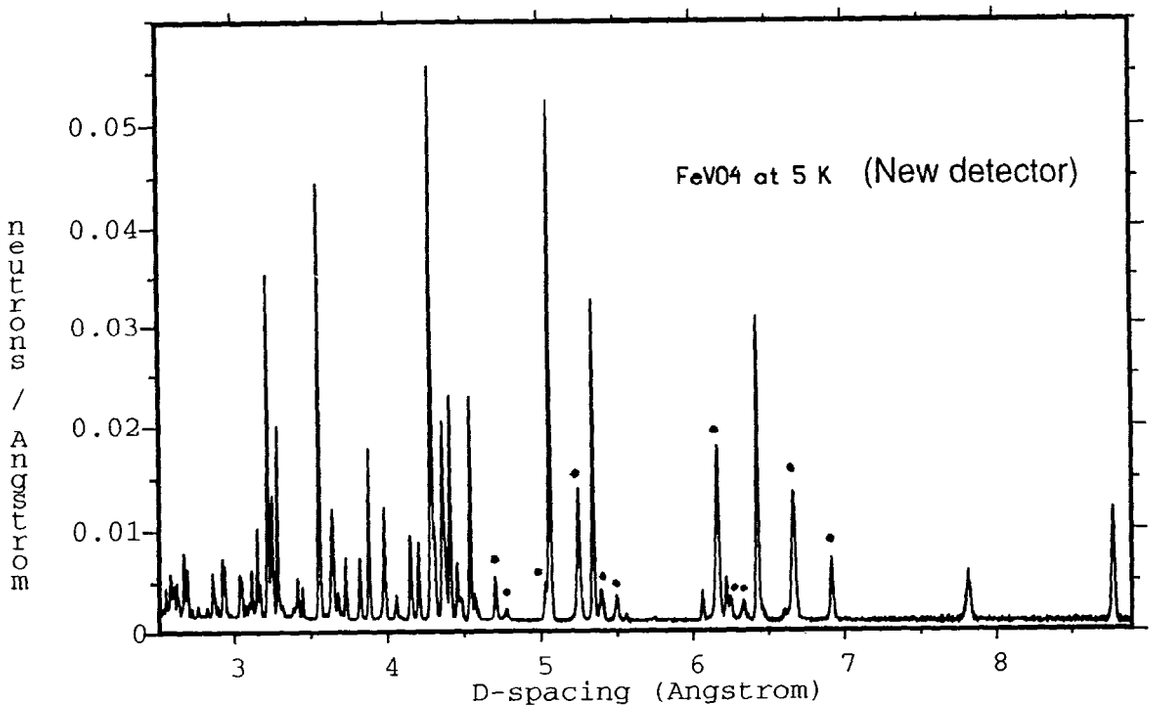

Figure 19: Magnetic ordering in $FeVO_4$ at 5K, taken on the inelastic spectrometer IRIS. The right hand edge of the spectrum corresponds to 18Å neutrons.

Long wavelength diffraction on pulsed sources is a very new area of work which promises much. In addition to the combined elastic and inelastic experiments and magnetic scattering examples above, other uses have included solution of "large" unit cell crystal structures and quality control of microgram samples of magnetic multilayers. More experiments are waiting to be done to further explore the potential of the technique.

8. Concluding Remarks

I am acutely aware that I have missed out much of importance in this rush through some of the highlights of the past few years of pulsed source science. This implies no value judgements. Reflectometry and liquids have only been touched upon, yet outstanding pulsed neutron science has been done in both areas. Single crystal diffraction - for which pulsed sources have major advantages, particularly in diffuse scattering studies - and small angle scattering - where the wide dynamic range is a big plus - have not even been mentioned. Perhaps the necessity to exclude so much just underlines the health and vigour of the science coming from pulsed sources, auguring well for the future.

A future which we are, of course, already preparing for. Discussions - both in Europe and the U.S.A - on a next generation pulsed source have raised the prospect of even more exciting new science, hopefully early in the next millennium. On a shorter timescale, new developments in instrumentation continue to widen the new science pulsed sources can tackle. For example, the design of the proposed MAPS instrument at ISIS was built on experience of utilising

existing instruments designed for powder measurements to tackle the difficult problems of efficient measurement of single crystal excitations.

We are still on not just one, but on several growth curves - of source strength, of instrumentation, and of learning how to exploit optimally this kind of source. Nethertheless, perhaps we now **can** say that pulsed sources have come of age.

9. Acknowledgements

This tour visited some of the high spots of pulsed sources as seen by me, but helped by Viktor Aksenov, Bruce Brown, Hiro Ikeda, Jim Jorgensen, Roger Pynn and many of my ISIS colleagues. The blame for the choice falls on me, the gratitude for producing so much to choose from goes to everyone else.

References

1. P A Egelstaff, in Advanced Neutron Sources 1988, ed. D. K. Hyer, Inst. of Physics, Bristol, p.881 (1989).

2. R Osborn, K A McEwen, E A Goremychkin and A D Taylor, Physica B **163**, 37 (1990).

3. R Osborn, E Balcar, S W Lovesey and A D Taylor, in Handbook on the Physics and Chemistry of Rare Earths, eds K A Gschneider and L Eyring, 1991.

4. T G Perring, G L Squires, A D Taylor, R Osborn and Z A Bowden, in ISIS 1989, ed. A D Taylor, Rutherford Appleton Laboratory, RL-89-050, 1989, p. A116.

5. A T Boothroyd, T G Perring, A D Taylor, D McKPaul and H A Mook, J. Magn. Magn. Mater. **104,** 713 (1992).

6. P W Mitchell, R T Heap and J R Lowden, in ISIS 1993, ed C C Wilson, Rutherford Appleton Laboratory, RL-93-050, 1993, p.A256.

7. S M Hayden, G Aeppli, R Osborn, A D Taylor, T G Perring, S W Cheong and Z Fisk, Phys Rev Lett **67**, 3622 (1991).

8. T G Perring, G Aeppli, C Broholm and S Lee, in ISIS 1993, ed C C Wilson, Rutherford Appleton Laboratory, RL-93-050, 1993, p.A261. See also p.83.

9. S E Nagler, D A Tennant, R A Cowley, T G Perring and S K Satija, Phys. Rev. **B44**, 12361 (1991).

10. T R Sosnick, W M Snow, P E Sokol, and R N Silver, Europhys. Lett. **9**, 707 (1989).

11. P Postorino, F Fillaux, J Mayers, J Tomkinson and R S Holt, J Chem. Phys. **94**, 4411 (1991). See also F Fillaux, J Tomkinson and J Mayers in ISIS 1993, ed C C Wilson, Rutherford Appleton Laboratory, RAL-93-050, 1993, p. A302.

12. See for example: W I F David, W T A Harrison, J M F Gunn, O Moze, A K Soper, P Day, J D Jorgensen, D G Hinks, M A Beno, L Soderholm, D W Capone II, I K Schuller, C U Segre, K Zhang and J D Grace, Nature **327**, 310 (1987).

13. See for example: I K Schuller and J D Jorgenson, Mater. Res. Soc. Bull, Jan 1989, P.27; J D Jorgensen, M A Beno, D G Hinks, L Soderholm, K J Volin, C U Segre, K Zhang and M S Kleefisch, Phys. Rev. **B36**, 3608 (1987).

14. W I F David, in Proc. MRS Symposium on Neutron Scattering for Materials Science, Boston, November 1989, eds M Shapiro, S C Moss and J D Jorgensen, MRS Proc. **166**, 41 (1990). W I F David, R M Ibberson, G A Jeffrey and J R Ruble, Physica **B180/181**, 597 (1992).

15. W I F David, personal communication. See also ISIS 1993, ed C C Wilson, Rutherford Appleton Laboratory, RL-93-050, 1993, p.11.

16. W I F David, R M Ibberson, J C Matthewman, K Prassides, T J S Dennis, J P Hare, H W Kroto, R Taylor and D R M Walton, Nature **353**, 147 (1991).

17. W I F David, R M Ibberson and T Matsuo, Proc. Roy. Soc. Lond. **A442**, 129 (1993).

18. S J L Billinge and T Egami, in Lattice Effects in High Tc Superconductors, ed. Y Bar-Yam, World Scientific 1992.

19. W F Kuhs, J L Finney, C Vettier and D V Bliss, J. Chem. Phys. **81**, 3612 (1984).

20. J D Jorgensen, R A Beyerlin, N Watanabe and T G Worlton, J. Chem. Phys. **81**, 3211 (1984).

21. H Takahashi, J D Jorgensen, B A Hunter, R L Hitterman, Shiyou Pei, F Izumi, Y Shimakawa, Y Kubo and T Manako, Physica **C191** 248 (1992).

22. J M Besson, J R Nelmes, J S Loveday, G Hamel, P Pruzan and S Hull, High Press. Res. **9**, 179 (1992).

23. R J Nelmes and J M Besson, in ISIS 1993, ed C C Wilson Rutherford Appleton Laboratory, RAL-93-050, 1993, p.97.

24. G L Povirk, M G Stout, M Bourke, J A Goldstone, A C Lawson, M Lovato, S R MacEwen, S R Nutt and A Needleman, Acta Metal. Mater. **40**, 2391, (1992).

25. A K Soper and J Z Turner, Int. J. Mod. Phys. **B7**, 3049, (1993).

26. A M Balagurov, G M Mironova, V E Novozchilov, A I Ostrovnoy, V G Simkin and V B Zlokazov, J. Appl. Cryst. **24**, 1009 (1991).

27. H Nojiri, M Motokawa, N Nishida and Y Endoh, Physica **B180/181**, 31 (1992).

28. M Mino, M Arai and M Motokawa, to be published.

29. U E Steigenberger, M Hagen and G Eckold, this proceedings.

30. B Bodmann et al, Phys. Lett. **B280**, 198 (1992). See also ISIS 1993, ed C C Wilson Rutherford Appleton Laboratory, RAL-93-050, 1993, p.51.

31. S W Harris, O Hartmann and R Hempelmann, J. Phys. :Condens Matter **3** 5665 (1991).

32. J Penfold and R K Thomas, J. Phys. :Condens Matter **2**, 1369 (1990).

33. A Inaba, T Shirakami, K Shibata, and S Ikeda, KENS Report -IX, Japan National Laboratory for High Energy Physics, 1993, p.186.

34. C J Carlile, I Mc L, Jamie, G Lockhart and J W White, Molec. Phys. **76**, 173 (1992).

35. J B Forsyth, C Wilkinson, C J Carlile and P S R Krishna, personal communication.